Materials Transactions, Vol. 46, No. 10 (2005) pp. 2237 to 2240

Fabrication of Fe-Based Bulk Amorphous Alloys Using Hot Metal and Commercial Ferro-Alloys

Seonghoon Yi[1,*], Ki Buem Kim[2] and Ho Sang Sohn[1]

[1]*Department of Materials Science and Metallurgy, Kyungpook National University, Daegu 702-701, Korea*
[2]*Technische Universität Darmstadt, FB 11 Material- und Geowissenschaften, FG Physikalische Metallkunde, D-64287 Darmstadt, Germany*

For commercial applications of Fe-based bulk amorphous alloys as structural materials, Fe-based bulk amorphous alloys that can be cost-effectively and massively produced have been developed using hot metal and ferro-alloys from a steel plant. The alloy $Fe_{68.0}C_{10.5}Si_{4.4}B_{6.5}P_{8.6}Al_{2.0}$ can be cast into a fully amorphous rod of 3 mm in diameter through a suction casting method. Upon heating the amorphous rod, a sequential crystallization behavior starting with the precipitation of fcc-Fe phase were observed. Since the crystallization kinetics was sluggish, the Fe-based bulk amorphous alloy can be used as a precursor for the fabrication of bulk nanostructured Fe alloy.

(Received June 13, 2005; Accepted August 8, 2005; Published October 15, 2005)

Keywords: *bulk amorphous alloys, bulk metallic glass, crystallization, suction casting*

1. Introduction

Bulk amorphous alloys exhibiting attractive properties for structural applications have been developed in many precious or refractory alloy systems.[1)] Recently, the development of Fe-based bulk amorphous alloy that can be cast into a fully amorphous rod of up to 12 mm in diameter has been reported.[2,3)] However, even after these significant progresses in the bulk amorphous alloy research, practical applications of bulk amorphous alloys seem to be still challenging. One of the main concerns for the practical applications can be cost-related. Most bulk amorphous alloys developed to date have been fabricated in a laboratory scale using high purity raw materials under clean atmosphere. Impurities in raw materials or slight oxidation during materials processing can significantly deteriorates the glass forming ability (GFA) of the alloys.[4)] Also, most bulk amorphous alloys contain large amounts of rare-earth or novel elements to enhance the GFA.[1–4)] Therefore, the production cost of bulk amorphous alloys is much higher than that of conventional crystalline alloys restricting extensive practical applications of bulk amorphous alloys. Nevertheless, some cast iron based amorphous alloys have been developed demonstrating Fe based bulk amorphous alloys can be prepared cost-effectively.[5,6)]

In this paper, cost-effective Fe-based bulk amorphous alloys have been developed using industrial raw materials supplied from a steel plant. Since carbon saturated hot metal is the main constituent, the Fe-based bulk amorphous alloys can be processed under commercial inert atmosphere allowing mass production at an affordable production cost. Moreover, through a relevant heat treatment procedure, the Fe-based bulk amorphous alloys can be evolved into nanostructured Fe-alloys with various microstructures. Therefore, the application fields of the Fe-based bulk amorphous alloys can be extended to the precursor for bulk nanostructured Fe alloys with tailored microstructures.

*Corresponding author, E-mail: yish@knu.ac.kr

2. Alloy Selection

The GFA of a Fe-based amorphous alloy is strongly dependent on the stability of liquid phase at low temperatures. That is, the liquid phase should be effectively undercooled to low temperatures so that the liquid structure can be frozen to amorphous structure due to low atomic mobility. Therefore, lowering of liquidus temperature is one of the main concerns in the alloy design for high GFA.[1)] It is well known that metalloids such as P, B, Si and C effectively lower the liquidus temperatures of Fe-based alloys. Since hot metal produced from blast furnace is a carbon saturated alloy with high content of P and Si, the melting temperature of hot metal is very low; about 1423 K. Therefore, hot metal having the composition shown in Table 1 was selected as the main constituent of the Fe-based bulk amorphous alloys.

3. Experimental

Small ingots of 10 g with desired compositions were prepared through an arc-melting process using a non-consumable tungsten electrode under Ar atmosphere. Optimum amounts of ferro-alloys that are currently used in a steelmaking plant were added to the hot metal for the preparation of ingots. The chemical compositions of the ferro-alloys were listed in Table 1. To assess the GFA of the

Table 1 Chemical compositions of ferro-alloys obtained from wet-chemical analysis.

(at%)	Fe	C	Si	B	P	Cr	Nb	W
Hot metal	79.7	18.0	2.3	—	—	—	—	—
Fe–Si	85.8	14.2	—	—	—	—	—	—
Fe–B (I)	47.7	—	1.2	51.1	—	—	—	—
Fe–P	61.9	—	3.7	—	34.3	—	—	—
Fe–Cr	39.0	6.1	—	—	—	54.9	—	—
Fe–Nb	54.1	—	—	—	—	—	45.9	—
Fe–W	50.4		—	—	—	—	—	49.6
Fe–B (II)	53.1	—	0.6	46.3	—	—	—	—

alloys, a piece of the ingot was levitation melted and quenched into a splat with the thickness of 50–80 μm in a splat quencher. Also, the ingot was re-melted and cast into a copper mold having the cylindrical cavity of various diameters through a suction casting method. The crystallinity and the GFA of the splats or the suction cast rods were estimated by X-ray diffractometer (XRD) and Differential scanning calorimeter (DSC), respectively. For crystallization study, fully amorphous rods ($\phi 2$) having the composition of $Fe_{68.0}C_{10.5}Si_{4.4}B_{6.5}P_{8.6}Al_{2.0}$ were heat treated at temperatures near T_g.

4. Results and Discussion

4.1 The GFA of hot metal based alloys

To enhance the GFA, optimum amounts of P, B and Si need to be added to the hot metal. Since each ferro-alloy has the fixed composition shown in Table 1, the nominal compositions of the alloys can be determined by the relative amount of each ferro-alloy added. Through a systematic alloy design procedure, the alloy with the composition of $Fe_{72.0}C_{14.3}Si_{4.8}B_{8.9}$ was prepared by the addition of optimum amounts of ferro-alloys to hot metal. Figure 1 shows the DSC heating curve with a heating rate of 0.667 K/s for the splat of the alloy $Fe_{72.0}C_{14.3}Si_{4.8}B_{8.9}$ exhibiting an exothermic event for crystallization of the amorphous phase. With the addition of P up to 7 at%, the exothermic peak splits into two exothermic peaks while the two exothermic peaks merge again with the addition of more than 8 at% P. Since the alloy $Fe_{69.4}C_{10.7}Si_{4.5}B_{6.6}P_{8.8}$ exhibited relatively large supercooled liquid region (ΔT_x) that is defined as the temperature interval between T_g and T_x, a 6th element was added to the alloy to enhance the GFA. In the selection of 6th element, the empirical rules for high GFA have been considered.[1] That is, as the atomic size difference and bonding force between constituent elements increases, the GFA of the alloy tends to increase. Based upon the literature data on the atomic radius and bonding force with the metalloids,[7] several elements were selected as the 6th element. Among them, some elements including Al, Nb, Mo, W, Cr and Ti were effective for the enhancement of GFA leading to the formation of fully amorphous rods of 1–3 mm in diameters (Figs. 2 and 3). Formation of fully amorphous phase in the rods can be confirmed by thermal analysis as well as microstructural analysis results. That is, the amounts of heat released during crystallization event of the amorphous rods were identical to those of ribbons in which fully amorphous phase was formed. Also, any crystalline phase could not be resolved through TEM analysis of the amorphous rods. With the small additions of Al less than 5 at%, the GFA as well as ΔT_x were significantly increased forming fully amorphous rod of up to 3 mm in diameter (Fig. 2).[8,9] The GFA was also increased effectively by the small amounts of some refractory elements (Fig. 3). As mentioned before, the raw materials used in this study are industrial grade materials in which certain amounts of impurities can exist. The impurities can either enhance or deteriorate the GFA of the alloys. Although all elements in the periodic table could not be analyzed in this study, the major impurities for each ferro-alloy were wet-analyzed as listed in Table 1. We believe that the impurity

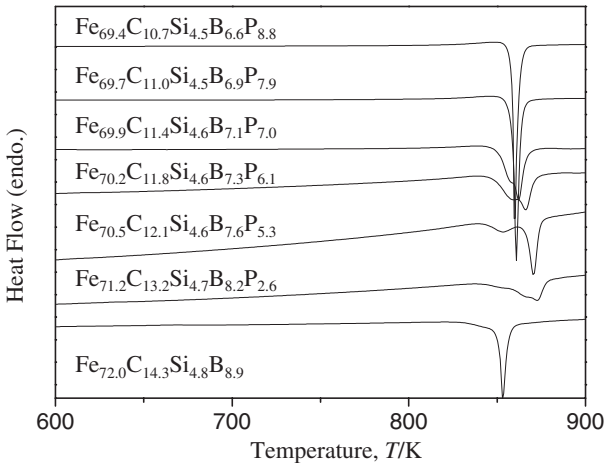

Fig. 1 DSC heating curves of the splat samples of the alloys in the multi-component system Fe–C–Si–B–P.

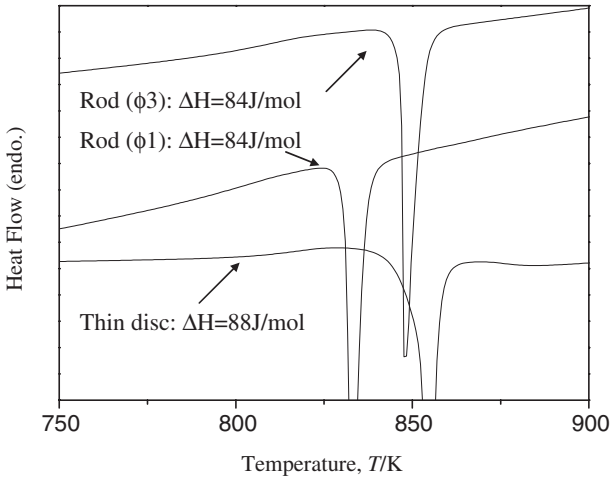

Fig. 2 DSC heating curves of the alloy $Fe_{68.0}C_{10.5}Si_{4.4}B_{6.5}P_{8.6}Al_{2.0}$: splat and the rods of 1 and 3 mm in diameters. The amounts of heat released during crystallization are identical within the experimental error range.

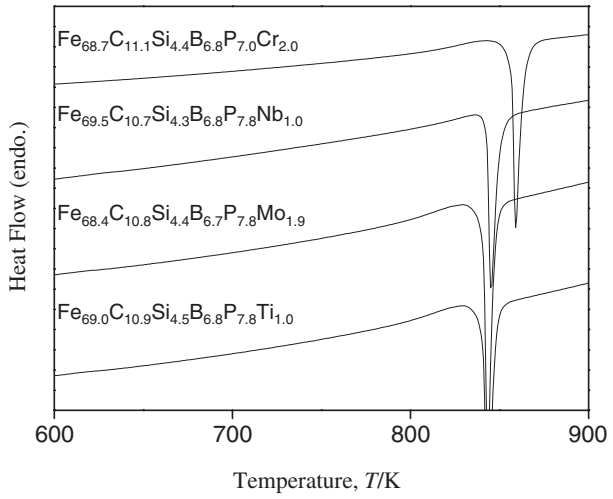

Fig. 3 DSC heating curves of the rods (ϕ1) with some refractory elements exhibiting fully amorphous nature of rods.

level in Table 1 would not significantly affect the GFA of the Fe-based bulk amorphous alloys developed in this study. Meanwhile, the alloys that can be cast into fully amorphous rods of larger than 1 mm in diameter can be massively produced as amorphous materials through strip casting or atomization process. Therefore, the amorphous alloys developed in this study may be practically applied as structural materials with superior properties as well as low production cost, leading to extended application of hot metal for valuable structural materials with high performance.

4.2 Crystallization behaviors of the alloy $Fe_{68.0}C_{10.5}Si_{4.4}B_{6.5}P_{8.6}Al_{2.0}$

Some materials processing routes have been proposed for the production of nanostructured Fe alloys.[10–12] However, cost-effectiveness and productivity can be critical issues for practical applications of the processes. Therefore, an alternating processing route using bulk amorphous alloys as precursors for nanostructured Fe alloys is of interest. That is, since the amorphous phase is not thermodynamically stable, the bulk amorphous alloys can be effectively transformed into bulk nanostructured alloys through a controlled crystallization process at low temperatures. Therefore, bulk nanostructured Fe alloys can be produced through relevant heat treatment processes of bulk amorphous alloys developed in this study. Understanding of crystallization behaviors upon continuous heating is important for the establishment of heat treatment strategy for nanostructured Fe alloys. As shown in Fig. 4, the single exothermic peak observed in DSC at high heating rate splits into two peaks as the cooling rate decreases, indicating a sequential crystallization behavior of the amorphous alloy $Fe_{68.0}C_{10.5}Si_{4.4}B_{6.5}P_{8.6}Al_{2.0}$. Figure 5 shows TEM bright field image and the corresponding selected area diffraction pattern from $Fe_{68.0}C_{10.5}Si_{4.4}B_{6.5}P_{8.6}Al_{2.0}$ alloy annealed at 783 K for 1.8 ks. The cuboid grains ranging from 20–40 nm in size were embedded homogeneously in the matrix. The corresponding selected area diffraction pattern shows the spotty ring diffraction peaks with the halo diffraction peaks typically obtained from the amorphous phase. The spotty ring diffraction peaks were identified as fcc Fe phase as marked in the Fig. 5(b). Figure 6 shows TEM bright field images (a and b), and the corresponding selected area diffraction patterns (c and d) from $Fe_{68.0}C_{10.5}Si_{4.4}B_{6.5}P_{8.6}Al_{2.0}$ alloy after heat treatment for 2.7 ks min at 783 K. The cuboid grains ranging from 20–40 nm in size were distributed homogeneously in the amorphous matrix as marked in the Fig. 6(a). The morphology and size of these cuboid crystals were similar to those of the fcc Fe phase, observed in Fig. 5(a). This indicates that the growth of the fcc Fe phase was very sluggish. Furthermore, the grain with 150 nm in size in Fig. 6(a) was distributed inhomogeneously through the sample. The corresponding selected area diffraction pattern was able to index to [021] zone axis of tetragonal Fe_3B phase. The bright field image in Fig. 6(c), obtained from another region of the sample, shows the dendritic morphology of the crystal with around 100–120 nm in size. The corresponding selected area diffraction pattern in Fig. 6(d) was identified as [112] zone axis of orthorhombic Fe_3C phase with the fcc Fe phase. Consequently, it is feasible to understand that the cuboid fcc Fe phase helps to crystallize the Fe_3C phase.

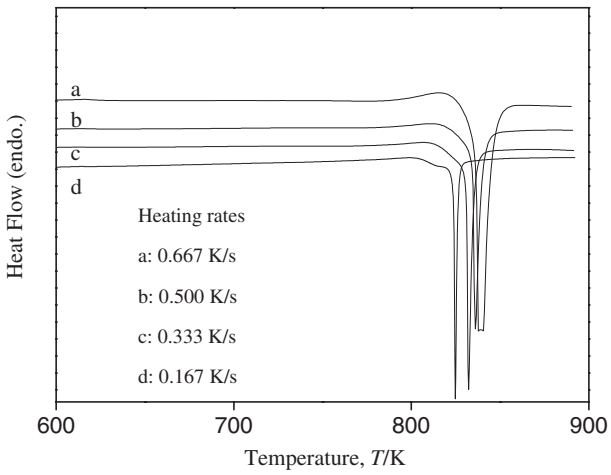

Fig. 4 DSC heating curves of the alloy $Fe_{68.0}C_{10.5}Si_{4.4}B_{6.5}P_{8.6}Al_{2.0}$ at different heating rates.

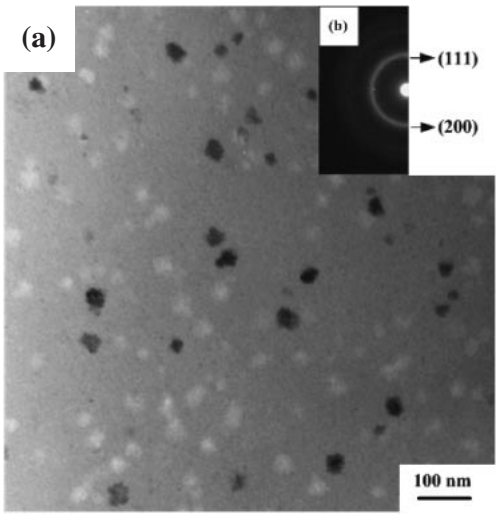

Fig. 5 TEM bright field image (a) and the corresponding selected area diffraction pattern (b) from $Fe_{68.0}C_{10.5}Si_{4.4}B_{6.5}P_{8.6}Al_{2.0}$ annealed at 783 K for 1.8 ks.

5. Summary

As structural bulk amorphous alloys that can be cost-effectively and massively produced, carbon saturated hot metal based bulk amorphous alloys have been developed using commercial hot metal and ferro alloys. Splat quenched amorphous ribbons can be prepared through optimum amounts of metalloid additions (B, P and Si) to hot metal. Some refractory elements as well as Al effectively increases the GFA of Fe–C–Si–B–P alloys, leading to the formation of fully amorphous rods of 1–3 mm in diameter.

Sequential crystallization can be observed upon heating the amorphous rod $Fe_{68.0}C_{10.5}Si_{4.4}B_{6.5}P_{8.6}Al_2$, staring with fcc ferrite precipitation followed by Fe_3C and Fe_3B precipitation. The grain growth kinetics was very sluggish, resulting in the formation of nanostructured bulk alloys through crystallization process.

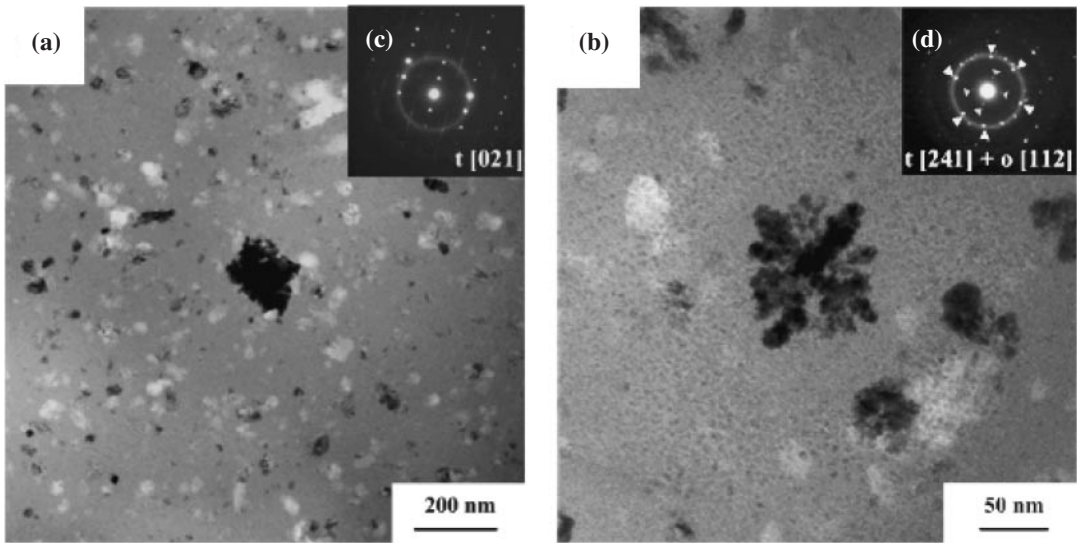

Fig. 6 TEM bright field images (a) and (b), and the corresponding selected area diffraction patterns (c) and (d) from $Fe_{68.0}C_{10.5}Si_{4.4}B_{6.5}P_{8.6}Al_{2.0}$ alloy after heat treatment for 2.7 ks at 783 K.

Acknowledgement

This work was financially supported by the Korean Ministry of Commerce, Industry, and Energy under the project named, "Development of structural metallic materials and parts with super strength and high performance."

REFERENCES

1) A. Inoue: Acta Mater. **48** (2000) 279–306.
2) A. Inoue, A. Takeuchi and B. Shen: Mater. Trans. **42** (2001) 970–978.
3) V. Ponnambalam, J. S. Poon and G. J. Shiflet: J. Mater. Res. **19** (2004) 1320–1323.
4) Z. P. Lu, C. T. Liu and W. D. Porter: Phys. Rev. Lett. **92** (2004) 245503.
5) X. M. Wang and A. Inoue: Mater. Trans. **40** (1999) 634–642.
6) M. Shapaan, J. Lendvai and L. K. Varga: J. Non-Cryst. Solids **330** (2003) 150–155.
7) F. R. De Boer, R. Boom, W. C. M. Mattens, A. R. Miedema and A. K. Niessen: *Cohesions in metals*, Amsterdam, The Netherlands: North-Holland (1988).
8) A. Inoue, Y. Shinohara and J. S. Gook: Mater. Trans., JIM **36** (1995) 1427.
9) A. Inoue and R. E. Park: Mater. Trans., JIM **37** (1996) 1715.
10) D. H. Shin, J. J. Pak, Y. K. Kim, K. T. Park and Y. S. Kim: Mater. Sci. Eng. A **323** (2002) 409–415.
11) R. Ueji, N. Tsuji, Y. Minamino and Y. Koizumi: Sci. Tech. Adv. Mater. **5** (2004) 153–162.
12) P. J. Maziasz, D. J. Alexander and J. L. Wright: Intermetallics **5** (1997) 547–562.